The retrospective prediction of ENSO from 1881-2000 by a hybrid coupled model – (II) Interdecadal and decadal variations in predictability

Ziwang Deng and Youmin Tang*

Environmental Science and Engineering,

University of Northern British Columbia,

3333 University Way, Prince George, BC, Canada, V2N 4Z9

Submitted to Climate Dynamics

Revised version

Corresponding author: Youmin Tang, E-mail: ytang@unbc.ca

Abstract

In this study, the retrospective predictions of ENSO (El Niño and Southern Oscillation) were performed for the period from 1881-2000 using a hybrid coupled model, which is an ocean general circulation model coupled to a linear statistical atmospheric model, and using a newly-developed initialization scheme of SST assimilation by Ensemble Kalman Filter (EnKF). With the retrospective predictions of the past 120 years, some important issues of ENSO predictability (measured by correlation and RMSE skills of NINO3 sea surface temperature anomaly index) were studied including decadal/interdecadal variations in ENSO predictability and the mechanisms responsible for these variations. Emphasis was placed on investigating the relationship between ENSO predictability and various characteristics of ENSO system such as the signal strength, the irregularity of periodicity, the noise and the nonlinearity.

It is found that there are significant decadal/interdecadal variations in the prediction skills of ENSO during the past 120 years. The ENSO events were more predictable during the late 19^{th} and the late 20^{th} centuries. The decadal/interdecadal variations of prediction skills are strongly related to the strength of sea-surface temperature anomaly (SSTA) signals, especially to the strength of SSTA signals at the frequencies of 2-4yr periods. The SSTA persistence, dominated by SSTA signals at frequencies over 4-yr periods, also has a positive relationship to prediction skills. The high-frequency noise,

on the other hand, has a strong inverse relationship to prediction skills, suggesting that it also probably plays an important role in ENSO predictability.

1. Introduction

Decadal variation in the ENSO variability has been found and documented in some literature (Kleeman et al. 1999; Gu and Philander 1997; Latif et al. 1998; Kirtman 1998; Hunt and Elliott 2003; Kiem and Franks 2004; Keith el al. 2004; Yeh et al. 2004; Zhang and Busalacchi 2005). Some studies suggested that this decadal variation is generated within the tropics , and is highly related to the decadal change in the zonal tilt of the equatorial thermocline (e.g., Munich et al. 1991; Jin et al. 1994; Timmerman and Jin et al. 2002; Timmerman et al. 2003; Rodgers et al. 2004). Some other studies connected it with the decadal variability of the mid-latitude atmosphere and ocean, linked by either atmospheric teleconnection or oceanic subduction of the subtropical gyre (Gu et al. 1997; Zhang et al.,1998; Kleeman et al. 1999; Barnett et al. 1999; Solomon et al.,2003). It has been found that anomalous surface water masses may subduct from the Northern and Southern Hemispheres toward the equator (e.g., Zhang et al.,1998; Solomon et al.,2003). Decadal variability in the mid-latitudes and subtropics of the Southern Pacific has also been found in both observation and model studies (Garreaud and Battisti, 1999; Linsley et al., 2000; Luo et al., 2001; Chang et al.,2001; Mantua and Hare, 2002; Folland et al.,2003).

Similarly, ENSO predictability also displays apparent decadal/interdecadal variations (e.g.,Balmaseda et al. 1995; Ji et al. 1996; Latif et al. 1998; Kirtman et al. 1998; Nakaegawa et al. 2004; Chen et al. 2004; Zhang et al. 2005). For example, while all models tend to have good

forecast skills in the 1980s, they had lower skills in the 1990s--- even with an improved initialization strategy (e.g., Chen et al. 1995; 1997; Jin 1996; Tang et al. 2004a). Mechanisms limiting ENSO predictability should be evaluated and significant progress has been made towards this goal in recent years. For example, it was suggested that the decadal dependence of predictability may be due to either the decadal changes in the mean state leading to the decadal variability of ENSO (e.g. Wang 1995; Zhang et al. 1999), or to the irregularity of ENSO related to nonlinear interactions within the tropical Pacific itself (e.g., Latif et al. 1998, Munnich el al. 1991; Jin et al. 1994; Chang et al. 1995; Chen 2004). Some studies also argued that the uncoupled atmospheric noise on monthly or seasonal mean time timescales might play a major role in the irregularity and predictability of ENSO (e.g., Battisti 1989; Kleeman and Power 1994; Blanke et al. 1997; Eckert and Latif 1997; Kleeman and Moore 1997). Further, Moore and Kleeman (1998), Kleeman and McCreary (1999), Kirtman et al. (1998) and Tang et al (2004b) discovered that the eigenmode amplitude of initial conditions controls prediction skills.

However, the variations of ENSO predictability and the mechanisms that underline the variations at decadal or longer timescales are not yet fully understood. Typically, there are two hypotheses to explain the loss of ENSO predictability with prediction lead time. The first argues that the loss of the predictability is due to the chaotic behavior of the coupled system (e.g., Chen et al. 2004), whereas the second attributes the loss of predictability to the stochasticity of the coupled system inherent to weather noise, and other high frequency variability such as the westerly wind burst and Maddan-Julian Oscillation (e.g., Moore et al 2006). To date, it is still not clear which regime plays a dominant role in controlling the variation of the ENSO predictability. One way to address these questions is to perform long-term ENSO retrospective predictions. Most of current

studies of ENSO predictability typically performed hindcasts for a period around 20-30 years due to the limited length of observations (e.g., Moore et al. 1998; 2006; Tang et al 2005), which makes it difficulty to derive statistically robust conclusions. Chen et al. (2004) performed a retrospective prediction covering 148 years, from 1856-2003, using the Lamont model. They found interdecadal variations in ENSO predictability. However, they did not explore in detail possible reasons of these variations in ENSO predictability. In addition, the fact that prediction skills are usually model dependent requires investigation of ENSO predictability using long-term hindcasts from other dynamical models.

This paper is the second part of our recent work on ENSO predictability. In the first part, we assimilated SST data for 120 years, from 1881-2000, into an oceanic general circulation model (OGCM) using an Ensemble Kalman Filter (EnKF) and obtained a skillful retrospective prediction of the 120 years (Deng et al. 2008). In this paper, we analyze the long-term hindcast. Emphasis is placed on examining decadal/interdecadal variations in ENSO predictability, as well as the relationship between the predictability and characteristics of ENSO variability such as the strength of the ENSO signals, the irregularity of periodicity, the noise and the initial-condition errors.

The paper is laid out as follows. The data, model and data assimilation scheme used in this study are briefly described in section 2. The results of prediction experiments and the variation of the predictability are examined in section 3. The observed equatorial SSTA characteristics responsible for the variations of predictability are discussed in section 4. The link between initial conditions and the predictability is presented in section 5. Finally, a summary and conclusion is included in section 6.

2. Data, model, initialization and diagnostic methods

2.1 Data, model and initialization scheme

In the first part of this work, we presented the data, model and initialization scheme in detail (Deng et al. 2008). Here we briefly review them.

The SST data used for verification and the construction of the statistical atmospheric model, as well for data assimilation, is from the monthly extended reconstructed global SST (ERSST.v2) dataset of Smith and Reynolds (2004), from 1854-2002 with 2^o lat. by 2^o lon. resolution**.** The statistical atmosphere is developed using monthly wind stress from the NCEP-NCAR reanalysis data set (Kalnay et al. 1996;Kistler et al. 2001), from January 1948 to December 2002.

The coupled model is identical to that used in Deng et al (2008), which is composed of an OGCM linked to a statistical atmospheric model. The ocean model is the latest version of Ocean Parallelise (OPA9.0, Madec et al. 1998). The domain of the model is the Pacific Ocean from 30°S to 30°N and 122°E to 70°W. The horizontal resolution in the zonal direction is 2^o while the resolution in the meridional direction is 0.5° within 5° of the equator, gradually changing up to 2.0° at 30°N and 30°S. There are 31 vertical levels with 17 concentrated in the top 250 m of the ocean. The time step for integration is 1.5 hours and the boundaries are closed.

The atmospheric model is a statistical method that uses model SST to predict contemporaneous wind stress. This statistical model was constructed using singular vector decomposition (SVD) with a cross-validation scheme that ensures no training data used in prediction periods. The initial conditions from which predictions start are from the SST assimilation of EnKF, as discussed in details in Deng et al. (2008).

2.2 Statistical diagnostic methods

Statistical methods used include wavelet transform (WT, Torrence,1998), fast Fourier transform (FFT), empirical orthogonal function (EOF) analysis, as well as a 20-yr running scheme similar to that used in John and Jeffrey (1999) to quantify ENSO persistence. Wavelet analysis is a tool for analyzing localized variations of power for a time series. By decomposing a time series into time-frequency space, one is able to determine both the dominant modes of variability and how those modes vary in time (Torrence et al. 1998). WT was employed to investigate the temporal variations of signal strength. As an efficient algorithm to compute the discrete Fourier transform (DFT) and its inverse, the fast Fourier transform (FFT) was used in decomposing original signal into different frequency-band components. A 20-yr running scheme is used to explore continuous variation of a variable of interest on a long time scale. For example, it can be used to explore decadal/indecadal variations in ENSO prediction skills. Here we calculate the skill in the first 20-yr window, say from 1881-1900, denoted at 1890. Then we move the window forward one year, from 1882-1901, to calculate the skill again, denoted at 1891. This process is repeated until the skill is calculated in the last window, from 1981-2000, denoted at 1990. Consequently, we can obtain a time series of 101 samples used to characterize the decadal/interdecadal variations in prediction skills. Similarly, we can apply this running scheme to any variable of interest to explore its variations at decadal or longer time scales. The use of the window length of 20-years is motivated by John and Jeffrey (1999) and Chen et al. (2004) where they investigated ENSO predictability every 20 years. In addition, the 20-yr length can allow us to have sufficent samples to derive

robust and stable conclusions. Unless otherwise indicated, we here refer to the above procedure as the " 20-yr running scheme" or "20-yr running".

3. Variations in prediction skills

The hindcasts were initialized from January 1881 to October 2000 at three months intervals (1 January, 1 April, 1 July, 1 October), and continued for 12 months. Thus we have 480 prediction cases each with up to 12 months lead. The prediction skill is evaluated using predicted NINO3 SSTA index against the observed counterpart. As usual, the skill is measured by correlation (R) and root mean square of errors (RMSE).

The overall prediction skill of 120 years initialized by the SST assimilation is presented in Fig. 1 (bold line), which is close to the skill of Chen et al. (2004), which indicated that the long-term retrospective prediction attained a useful skill. Shown in Fig. 2 is a comparison of predicted NINO3 SSTA of 6-month leads against the observed counterpart from 1881-2000. As can be seen, the prediction can reasonably well capture most ENSO events at the 6-month leads although it sometimes produced false alarms or under-predicted the intensity. At 9- and 12-month leads, the prediction still displayed the ability to capture many ENSO events (not shown).

Our interest here is to investigate decadal/interdecadal variations in ENSO predictability. Thus, we also calculated the prediction skill of six 20-yr sub-periods each as in Chen et al. (2004), as shown in Fig. 1. It is apparent that the prediction skill varies from one sub-period to another sub-period. Except for 1921-1940, the correlation skill is greater than 0.5 at the 6 month leads. If the correlation coefficient of 0.5 is chosen as a

criteria of skillful forecast[1], the longest lead time that still has the skill is 12 months for 1981-2000, 9 months for 1881-1990, 7 months for 1961-1980, 6 months for 1901-1920 and 1941-1960 and 5 months for 1921-1940.

The RMSE skill shown in Fig. 1b displays many features similar to Fig. 1a although some discrepancies exist between them. For example the periods of 1881-1900 and 1961-1980 that have good correlation skills also have relatively small RMSE whereas the periods of 1901-1920, 1921-1940 and 1941-1960 that have low correlation skills correspondingly have high RMSE. A special case is the period 1981-2000, which has high correlation but large RMSE. This is due probably to very strong ENSO variability anomalies during this period (also see following sections).

Comparing Fig. 1 with a similar figure of Chen et al. (2004), it was found that the decadal/interdecadal variations in the predictability here are consistent with theirs, although the models have some differences in the skill and the division of sub-periods, suggesting that such variations may not be model dependent.

The decadal/interdecadal variations in ENSO predictability are further detected by the 20-yr running scheme. The variation of correlation and RMSE skills of NINO3 SSTA index at the lead time of 6-months from 1881-2000 are shown in Fig.3a (thick- solid line) and Fig.3b respectively. As can be seen, there are significant decadal/interdecadal variations in both correlation and RMSE skills. The prediction skills are good in the beginning and end of the period, while the skills are poor during the period around 1916-1944. If the correlation coefficient of 0.5 is considered as a useful skill in ENSO

[1] The correlation was calculated using samples of 20-yr period, thus the criteria of its statistical significance would be 0.22 at the confidence level of 95% if the samples used were independent. However due to a high persistence, the Pacific SSTA is of non-zero trend and autocorrelated time series, serial correlation must be considered when a statistically significant test is performed (Ebisuzaki 1997).

prediction, the prediction during this period has no skill. Such a striking decadal/interdecadal variations in the predictability are also reflected by the fact that the prediction skill continuously decreases from 1900-1925 but increases from 1940 to 1960.

4. Impact of ENSO features on the predictability.

As shown in the proceeding section, there are significant decadal/interdecadal variations in ENSO predictability. One challenging question is what causes these variations of predictability? In this section, we will explore this issue. As discussed in the introduction, ENSO predictability might be dependent on such ENSO characteristics as its frequency, amplitude, irregularity and periodicity. Hence, emphasis will be placed on investigating the relationship between the predictability and these ENSO features.

4.1 The predictability and the strength of ENSO variability

We first explore the relationship between the predictability with the strength of ENSO variability. There are several methods to measure the strength of ENSO variability using the observed SSTA. The first is to use the variance of the NINO3 SSTA index (referred to as V_NINO3 hereafter), which characterizes the amplitude of ENSO variability. The second is the variance contribution accounted for by the first EOF mode of tropical Pacific SSTA, since the spatial structure of the first EOF mode is always an ENSO-like pattern. It should be noticed that the EOF analysis, as a linear statistical method, only describes stationary oscillations. Thus the first EOF mode, which changes signs between El Niño and La Niña events, only characterizes the linear component of ENSO and is unable to describe the asymmetry in the spatial pattern between average warm and cold events (Monahan 2001, 2004). In the following discussions, the variance explained by the first EOF mode, denoted by VPC1, is used to measure the strength of the linear

component of ENSO variability.

V_NINO3 and VPC1 from 1881-2000, obtained using the "20-yr running scheme", are well correlated, with a correlation coefficient of 0.76. This suggests that the strength of ENSO variability is mainly from the contribution of its linear component. It should be noted that there is a very good agreement between VPC1 and V_NINO3 from 1890-1940. This is due partly to the method used to reconstruct the historical SST data. The observations are sparse during this period. Thus, spatial SST patterns were reconstructed by fitting these data to a set of spatial modes (Smith and Reynolds, 2002, 2004).

Significant decadal/interdecadal V_NINO3 variations can be found in Fig. 3a (thin-solid line), for example, low values during 1915-1945 and high amplitudes during other periods. Torrence et al (1998) also found a 15-year modulation of variance in the tropical Pacific SST field. Such decadal/interdecadal variations in the strength of ENSO variability are related to the ENSO predictability. A scatter plot illustrating the relationship between the correlation skill of 6-month lead predictions and ENSO strength is shown in Fig. 4. Fig. 4a shows a nearly linear relationship between VPC1 and the prediction skill (drawn in circle) with a high correlation coefficient of 0.88. When the VPC1 is large the prediction skill is high and vice versa. Fig. 4a also shows a linear relationship between the predictability and V_NINO3 (see asterisk), with a correlation coefficient of 0.74. As discussed above, the VPC1 characterizes the strength of the linear ENSO component while V_NINO3 characterizes the full ENSO signal. Thus, much of the ENSO predictability may be from the successful predictions using linear methods.

Fig. 4b is the same as Fig. 4a but uses RMSE instead of the correlation to measure prediction skill score. Fig. 4b shows that a small VPC1 often leads to a poor prediction

skill (i.e. large RMSE). When the VPC1 is large, the RMSE is more variable (see circle). This differs from Fig. 4a, which shows a more linear relationship between predictability and the strength of ENSO. Fig. 4b shows a more complicated relationship between RMSE and V_NINO3 (see asterisk), which may be due to the nature of RMSE. Usually the predictions of weak events with small amplitude generate small RMSE, even though their correlation skill is poor. In addition, there are other factors impacting ENSO predictability, which we will analyze below.

4.2 Persistence

The tropic equatorial Pacific SSTA has strong persistence and variations in persistence might strongly affect ENSO prediction skill. To explore this, we calculated respectively the skills of persistence predictions of the NINO3 SSTA index with leads times of 3-, 6-, 9- and 12- months, for the period from 1881-2000 using the 20-yr running scheme. It was found that these skills have similar temporal variations. The correlation skill of persistence prediction at 6-month leads (dashed thin-line shown in fig.3), shows striking decadal/interdecadal variations. Comparing the persistent skill and the model correlation skill (thick solid line) reveals that the decadal/interdecadal variations of persistence skill and decadal/interdecadal variations of predictability have many similar features. For example, a low persistence during 1920s-1940s and 1970s corresponds with a poor correlation skill of predictions. The correlation coefficient between persistence and the correlation skill is 0.57 which is statistically significant at the confidence level of 99%. This suggests that persistence is a key factor in control of decadal variations of ENSO predictability.

The good relationship between persistence and predictability might explain why the

predictability is not too low around the 1910s and 1950s when there were weak SSTA signals at the frequencies of 2-4 yrs and relatively strong noise of high frequencies (also see next subsection and Fig. 5). In subsection 4.3, we show that ENSO predictability are greatly influenced by the strength of the ENSO signals at periods of 2-4 yrs.

4.3 Periodicity

The predictability of a dynamical system may be related to its periodicity. To examine the possible relationship between ENSO predictability and periods of ENSO variability, wavelet transformation was used to analyze temporal variations in significant periods of the NINO3 SSTA index. The wavelet power spectrum of observed NINO3 SSTA index is plotted in Fig. 5a. It displays the strength of signals in time-periodicity space. As can be seen, the significant periods vary from time to time, ranging from 2-4 yrs for 1885-1905, 5-8 yrs for 1905-1928 and 1945-1963, 1.5-4yrs for 1963-1976, and 4-6yrs after 1980. For the period from 1928-1945, there are only a few times with significant signals over periods between 1- 2.5yrs. In addition, during the first half of the 1980s and second half of the 1990s, there are also significant signals over periods of 1 to 4yrs.

Comparing the variation of correlation skill at the 6-month lead (Fig. 3) and the variation of significant periods (Fig. 5a) reveals that good prediction skill often occurred in times with significant periods of 2-4 yrs, such as 1885-1905, the first half of 1980s and the second half of 1990s. Low skills were attained in times with significant periods of less than 2 yrs. One might argue that the above results are model dependent, and related to the characteristic periods of the model itself, since a high predictability could be expected during times when the characteristic periods of the model match the observed ENSO periods. That might be true since the coupled model used here has the

characteristic period of 33 months. However other ENSO models that have different characteristic periods also have decadal/interdecadal variations in predictability similar to Fig. 3 (e.g., Zhou et al. 2007; Chen et al. 2004), suggesting that the above findings are probably not model dependent. On the other hand, most ENSO prediction models have the characteristic periods of 3-5 yrs, leading to their failure in capturing realistic ENSO signals beyond 3-5 yrs. This may explain why most ENSO prediction models can attain good prediction skills for the first half of 1980s and the second half of 1990s that had a realistic period of 3-5 yrs, and poor skills for the period of the first half of 1990s, which had a significant period greater than 5 yrs (Fig. 5a). Figure 5a also shows that there is a strong high-frequent variation with periods less than half a year during 1920-1955, which may explain why there was relatively low predictability during this period.

To further analyze the relationship between the period and prediction skill, we decomposed the NINO3 SSTA index into six independent period bands by means of FFT and inverse FFT. The six period bands are < 3month; 3-6month; 6-12month; 1-2year; 2-4year and >4year. They explain respectively 2.11%, 3.61%,4.38%,15.85%,34.69% and 39.36% of the total variance. Shown in Table 1 are the correlation coefficients between the variance of these components and prediction skills of 6-month leads, obtained using the 20-yr running scheme, indicating the impact of strength of ENSO variability of different frequencies on the predictability. Table 1 shows that the ENSO predictability is related to the strength of the components of SSTA variability in two frequency bands: 2-4 yrs and under 3-months. The former has a strong positive relationship with the predictability whereas the latter has a significant negative correlation with the predictability, indicating that the strength of SSTA signals at the frequency of both 2-4

yrs and less than 3 months control much of the variation of predictability. As discussed in section 4.1, the predictability is highly associated with the strength of ENSO signals. A number of previous studies also showed a strong connection between ENSO predictability and its amplitude (e.g., Kirtman and Schopf, 1998; Kleeman and McCreary 1999; Moore and Kleeman 1999; Tang et al. 2004; 2005; Chen et al. 2004; Tang et al. 2007). The results shown here address the importance of specific frequencies of ENSO signals to ENSO predictability, further enhancing this understanding.

Fig. 6 shows changes in predictability with the signal variance in different frequency bands. Consistent decadal/interdecadal variations can be found in both predictability and in the variance of frequency bands of 2-4 yrs, as shown in Fig. 6b, with strong correlation coefficients between them, as shown in Table 1. However, the variance in frequency bands of 2-4 yrs does not explain the decadal or smaller time scale changes in predictability. The signal variance for periods greater than 2-yrs almost perfectly fits changes in predictability in both interdecadal and smaller time scale variations, as shown in Fig. 6a. The correlation coefficient between the correlation skill and the variance in Fig. 6a is 0.89, considerably higher than its counterpart of Fig. 6b. This suggests that the interdecadal changes in predictability might be mainly related to the signals of 2-4 yr periods whereas the decadal or smaller time-scale changes in predictability are more related to longer-period signals. This also explains why there is a very small correlation coefficient between the predictability, which is dominated by the signals of the 2-4 yr periods, and the variance of the signals over the 4-yr periods as shown in Table 1.

The strong negative correlation between the predictability and the strength of high-frequency signals, found in the under 3-month periods, suggests a significant impact of

noise on the predictability. As shown in Fig. 6c, when the high frequency signals (noise) are strong the predictability is low (low correlation and high RMSE) and vice versa. It has been argued in literature that the noise may be a major limitation to ENSO predictability (e. g., Penland and Matrasova 1994; Kleeman and Moore 1997; Thompson and Battisti 2000; Moore et al. 2006; Flügel et al.2004), which is also confirmed by Fig. 6c. However, it should be noted that the coupled model used here incorporates a noise-free statistical atmospheric model, and the noise was here diagnosed only from observed SST data. Thus the above results mainly reflect the variations of ENSO predictability under a realistic SST noise background. The noise in SST observations increases the uncertainty in the initial conditions through SST assimilation, which could affect the predictability. However, it is not clear how much of observed noise can be brought into the coupled model and, in turn, impact on prediction skills by data assimilation. To understand the role of noise in ENSO predictability, a fully coupled GCM may be required. Nevertheless, the finding shown in Table 1 shed light on the importance of noise to ENSO predictability although the complete understanding of its impact on ENSO predictability needs further study.

5. Impact of initial conditions on the predictability

The initial conditions play an important role in ENSO prediction skills. ENSO prediction is an initial value problem, and the further evolution of the system depends highly on the initial state from which it started. In last section, we found the decadal/interdecadal variations in ENSO predictability are highly related to the variations of observed ENSO signals. The observed signals are incorporated into this coupled model through initial conditions. It is interesting to examine whether there are significant

decadal/interdecadal variations in initial conditions that in turn affect the decadal/interdecadal variations in predictability, especially using a long-term retrospective prediction over 100 years. In this section, we will analyze the errors and structure of SST, surface zonal current and thermocline depth at the initial time, and then explore their relationships with predictability.

The initial conditions were generated by SST assimilation forced by the reconstructed wind stress, as described in Deng et al. (2007). Fig 5b shows the wavelet power spectrum of modeled NINO3 index, displaying a pattern very similar to Fig. 5a. In the preceding section, we discussed the relationship between ENSO predictability with significant observed characteristics of SSTA variability. However compared with Fig. 5a, Fig.5b shows stronger interannual signals and weaker high frequent signals at the period smaller than half a year (see the test curve at the right side), suggesting that the ocean model acts as a low-pass filter to filter the high frequency components. Since the analyzed SSTA NINO3 index is in very good agreement with its observed counterpart, with a correlation of 0.95 for the period from 1881-2000, the findings and conclusions derived from the observed NINO3 SSTA index in last section also hold here (not shown). Therefore, we will address the effects of model errors, zonal current and heat content of the upper ocean on the predictability in this section. These have not been addressed in previous studies.

5.1 The initial errors in SST

Initial conditions always contain uncertainties, which affect model prediction skill. In this section, we discuss the variation of initial errors and their affects on the variations of predictability at decadal or longer time scales.

To explore the impact of initial conditions on the decadal/interdecadal variations of prediction skills, we first analyze the accuracy of initial conditions relative to observations. Fig. 7a is correlation skill of the analyzed NINO3 SSTA index against the observed counterpart, obtained using the 20-yr running scheme. Fig.7a is very similar to the correlation skill of 6-month leads (Fig 3a) with their correlation of 0.91, indicating the important impact of initial conditions on predictability.

The other interesting finding is that model RMSE normalized by the standard deviation of observed NINO3 is inversely correlated with correlation skill (Fig. 7a) with a correlation coefficient of -0.95, as shown in Fig. 7b. This ratio is obtained by the 20-yr running scheme and can be understood as the relative RMSE. The relative RRMSE has a good relationship with the prediction skill of 6-month leads (Fig. 3a) with a correlation of -0.79. However, the RMSE itself only has a weak correlation of -0.21 with the prediction skill of 6-month leads, indicating the importance of the strength of ENSO signals in influencing ENSO predictability as discussed in section 4.1.

One interesting question raised from Fig. 7 is whether the dedacal/interdecadal variation in predictability is mainly due to assimilation quality. To explore this issue, we repeated the long-term retrospective prediction of the past 120 years initialized from the control run without SST assimilation. It was found that the prediction skill initialized from the control run is quite low compared to the skill by data assimilation (see part I, this issue), but still displayed striking decadal/interdecadal variation similar to that shown above, suggesting that the dedacal/interdecadal variation in predictability is not due to the quality of data assimilation. In fact, a careful look at Fig. 7a found the range of the amount of the correlation skill is small, with the maximum of 0.97 and minimum 0.923

indicating the assimilation quality is uniformly good during the whole period. It is the same for RMSE skill with the maximum value of 0.15 against the minimum value of 0.09 (not shown).

The relative low skill from 1925–1955 in Fig 7 is due mainly to relatively weak signals and strong noises during this period, as shown in Fig. 5a, displaying weak signals of a 2-4 yr period and strong signals of a less than 6-month period. The strength of signal and noise of observations will influence the assimilation performance, leading to the relative variation of assimilation skill during different periods.

5.2 Surface zonal current and thermocline depth

The surface zonal current and thermocline depth will be explored in this subsection. The former is a dynamical variable whereas the latter describes the thermodynamical structure in the upper ocean. The role of thermocline disturbance in the formation and development of El Niño has been addressed. For example, Hasegawa and Hanawa (2003) indicated that the entire equatorial heat content anomaly (HCA) leads the Niño-3 index anomaly by about a quarter (about 3 years) of the period of the decadal variability in the tropical Pacific. This time lag of a quarter of the period is consistent with the idea of the "recharge oscillator" model for ENSO dynamics. McPhaden (2003) argued that the initialization of upper ocean heat content variations might lead to seasonally varying enhancements of forecast skill, with the most pronounced enhancements for forecasts starting early and late in the development of ENSO events. It was also found that there are significant relationships between the surface current anomaly pattern and SSTA over the tropical Pacific (e.g., Yu et al. 2003; Tang et al. 2004a).

The EOF analysis was performed for the surface zonal current anomaly (UA) and thermocline depth anomaly (Z20A) for the period from 1881-2000. Here we used the depth of 20℃ isotherm to denote the thermocline depth. The first modes of UA and Z20A, accounting for 61.9% and 66.8 % of total variance respectively, are shown in Fig 8b and Fig 8c. The EOF1 of UA is characterized by a uniform variation over the Pacific basin along the equator whereas EOF1 of Z20A is characterized by a dipole pattern spanning over the east-west equatorial Pacific Ocean. Such a dipole pattern describes a typical La Niña phase as shown in Fig. 8a, namely that, warm water piles on the western side of Pacific due to the increase of easterly wind in the central and western Pacific. The spatial pattern of EOF1 of UA is similar to that of SSTA (Fig. 8a). This is because the model's zonal current is driven by wind stress that is controlled by SSTA. The time series of the two EOF1 modes are highly correlated with the simulated NINO3 SSTA index (correlation coefficient of -0.89 for UA and -0.86 for Z20A), and with the time series of EOF1 of SSTA (correlation coefficient of 0.94 for both).

Fig. 9 is the variance contribution of EOF1 derived from the SSTA, UA and Z20A, obtained using the 20-yr running scheme, i.e., EOF analyses were performed in each running window of 20-yrs from 1881-2000. These variances show strikingly consistent decadal/interdecadal variations that are related to the variations of the predictability. The correlation coefficients of the prediction skill (correlation) at 6-month leads to these variances are 0.67, 0.71 and 0.66 respectively.

5.3 Zonal tilt of the equatorial thermocline

Timmermann (2002) and Rodgers et al. (2004) found that decadal modulations of the amplitude of ENSO are associated with decadal changes in zonal tilt of the equatorial

thermocline, and the strong ENSO events often occur when the tilt is anomalously low. We also examined the possible relationship between the zonal tilt of the equatorial thermocline and ENSO predictability. Here the zonal tilt is defined as below

$$Z20\_Tilt = Z20'_W - Z20'_E$$

where $Z20'_W$ is the averaged normalized Z20 over the region of 2°S-2°N and 156°E-160°E and $Z20'_E$ is the averaged normalized Z20 over the region of 2°S-2°N and 110°W-106°W. The two regions were selected because they have the maximum standard deviation. We used normalized $Z20'$, not raw Z20, to define the zonal tilt since the thermocline depth always has stronger anomalies in the east than in the west.

The wavelet spectrum of Z20_*Tilt* shown in figure 5c is very similar to that of observed SSTA. The variance of Z20_*Tilt* (not shown) and the variance of UA in Fig. 9 have a strong linear relationship with a correlation coefficient of 0.88. This is not surprising since the west-east tilt of the thermocline is highly related to the structure and distribution of the upper oceanic currents, as explained by the recharge oscillator theory (Jin 1997, 1999). The correlation between the variance of the zonal tilt and the prediction skill (correlation) is 0.64. However, we did not find a significant relationship between the mean Z20_*Tilt* and the prediction skill.

In summary, in addition to decadal/interdecadal variations in observed SSTA, both model dynamical and thermodynamic variables of the initial fields reflect the decadal/interdecadal variability. These decadal/interdecadal signals present in the initial conditions greatly affect the prediction skills and, in turn, lead to the decadal/interdecadal variations in the predictability.

6. Summary and discussion

It is important in ENSO predictability studies to perform long-term retrospective predictions that cover a sufficient number of ENSO cycles, from which robust conclusions can be derived. Chen et al. (2004) explored the possibility using the Lamont model and found that ENSO predictability has striking decadal/interdecadal variations. This paper expanded on their work using a different ENSO model, and in particular explored possible reasons responsible for the decadal/interdecadal variations in ENSO predictability that Chen et al. (2004) did not address.

It was found that ENSO predictability in our model shows consistent decadal/interdecadal variations with those in the Lamont model. Namely, the prediction skills were high in the late 19th century from 1881-1900, declining with time to a minimum around 1940-1950s, and then increasing with time until the 1960s. This model had a relatively good prediction skill from the 1960s, especially in the late 20th century from 1881-2000, as in Chen et al. (2004). Recently we also completed a set of long-term retrospective predictions using a hybrid coupled model (Tang and Hsieh 2003), and found nearly identical features of ENSO predictability (Zhou et al. 2007). These similar results indicate that the decadal/interdecadal variability in ENSO predictability exists generally, and is not model dependent.

Possible reasons responsible for decadal/interdecadal variations in ENSO predictability were investigated in detail through diagnosing SST observations and the analyzed oceanic assimilation fields including SST, surface zonal current and thermocline depth. Emphasis was placed on exploring the impact of significant features of ENSO on predictability. It was found that interdecadal variations in predictability are in good agreement with interdecadal ENSO variability. In the late 19th century, the model had a

high correlation and a low RMSE skill when ENSO variability was strong. ENSO variability was relatively weak from 1910s-1960s, during which the model showed coincidentally the poorest prediction skill. The middle-late 20th century had the best prediction skill, associated with the strongest ENSO variability. In particular, the interdecadal variation in predictability might be mainly related to the strength of the signals of the 2-4 yr periods whereas the decadal or smaller time-scale variation in predictability is probably related to the strength of the signals with periods of over 4-yrs. Such a good relationship between the strength of ENSO variability and predictability was also found in the Lamont model (Chen et al. 2004), indicating the critical impact of signals present in initial conditions.

The strong signals present in initial conditions are able to resist dissipation by stochastic or chaotic components of the system, leading to good persistence skill. Thus a good relationship between decadal/interdecadal variations in ENSO predictability and persistence of NINO3 SSTA existed, as expected. It should be noticed that the persistence skill of NINO3 SSTA is not strongly related to the signals of all frequency bands of ENSO. It is mainly related to signals with periods of over 4-yrs. The signals with 2-4 yr periods contribute little to 6-month lead persistence skill.

Another factor that impacts ENSO predictability is high-frequency noise, with periods of less than 3-months. It was found that there was a strong inverse relationship between decadal/interdecadal variations in ENSO predictability with the strength of noise. The results shown here supports a popular hypothesis of predictability, that noise limits ENSO predictability (e.g. Karspeck et al. 2006). It is especially true when the ENSO signals present in initial conditions are not strong.

Further analyses of initial conditions produced by SST observations show that the decadal/interdecadal variations are also reflected in surface currents, thermocline depth and the east-west tile of thermocline, all of which show consistent decadal/interdecadal variations associated with ENSO predictability. These results further indicate that the decadal/interdecadal variations of ENSO predictability are due mainly to decadal/interdecadal variability of the tropical Pacific. Theoretically, the west-east tile of thermocline determines the strength of ENSO variability. If we calculate the mean state (e.g. NINO3 SST) of the tropical Pacific using the 20-yr running scheme, it can be found that the variation of the mean state also clearly shows decadal/interdecadal variations. Those variations are similar to those in ENSO predictability (not shown), suggesting that the decadal/interdecadal variations of ENSO predictability are probably caused by the variation of the mean state of the tropical Pacific, verifying some earlier findings (e,g., Wang et al. 1999; 1995). This is an important verification since there had been no evidence from a long-term realistic ENSO prediction to support this conclusion.

An interesting finding is that the initial errors of predictions also displayed decadal/interdecadal variations which were highly related to ENSO predictability. It is not clear what caused the decadal/interdecadal variations in initial errors. In this study, the initial conditions were generated by the assimilation of SST observations, and the initial errors were measured by SST itself. Thus, one possible reason for the decadal/interdecadal variations in initial errors is due to the variation of the strength of SST signals. When the signals present in SST observations were strong, a better assimilation was achieved, leading to small initial errors, whereas when the signals were weak, the assimilation was probably poor because there was relatively more noise in the

observations. Thus, the strength of ENSO signals is probably the most important factor explaining ENSO predictability.

It should be noted that several concerns should be born in mind. First, the quality of the historic SST data changes from time to time. As indicated by Smith and Reynolds (2002, 2004), the SST observations were sparse before the 1940s. However the fact that a high predictability also occurred in the early 19th century and similar results were found in Chen et al. (2004), which used another historic SST dataset, suggests that the data quality is not a source of decadal/interdecadal variations in ENSO predictability. Second, we have used running windows each having 20 years to analyze decadal/interdecadal variations in predictability and in control variables, which is somehow subjective. The window length of 20 years was motivated by Chen et al (2004) where the decadal/interdecadal variations in predictability were discussed every 20 years. We also performed several sensitivity experiments, i.e., using a window length of 10-yrs, 30-yrs and 40-yrs. The relationships of predictability to signal and noise are similar using those other time windows. Lastly, we used a 3-month high-pass filter to obtain the noise data. One may argue that this is not very objective. For example, maybe 1-month or 2-month high-pass filters can generate noise that is more realistic. In addition, we only examined the noise in SST analysis, and did not consider the noise in other variables such as oceanic currents and thermocline. These concerns need to be clarified through analyses that are more comprehensive. Nevertheless, this is to date the second work discussing ENSO predictability using a long-term hindcasts, and it further verifies the findings in Chen et al. (2004). In particular, this is the first study to explore reasons for

decadal/interdecadal variations in ENSO predictability using a long-term retrospective ENSO prediction, which shed lights on some important issues of ENSO predictability.

Acknowledgements

We are grateful to Dr.Tom Smith for detailed comments on the original manuscript. This work was supported by Canadian Foundation for Climate and Atmospheric Sciences (CFCAS) Grant GR-523.

References:

Balmaseda, M. A., Davey, M. K., and Anderson, D. L. T., 1995: Decadal and seasonal dependence of ENSO prediction skill, *J. Climate*, **8**, 2705– 2715.

Barnett, T.P., D.W. Pierce, R. Saravanan, N. Schneider, D. Dommenget, and M. Latif, 1999: Origins of midlatitude Pacific decadal variability. Geophys. Res. Lett., 26, 1453-1456.

Battisti, D. S., and A. C. Hirst, 1989: Interannual variability in the tropical atmosphere–ocean system: Influence of the basic state, ocean geometry, and nonlinearity. J. Atmos. Sci., 46, 1687–1712.

Blanke, B., J. D. Neelin, and D. Gutzler, 1997: Estimating the effect of stochastic wind stress forcing on ENSO irregularity. J. Climate, 10, 1473–1486.

Chang, P., L. Ji, B. Wang, and T. Li, 1995: Interactions between the seasonal cycle and El Niño–Southern Oscillation in an intermediate coupled ocean–atmosphere model. J. Atmos. Sci., 52, 2353–2372.

Chang, P., B. S. Giese, L. Ji, and H. F. Seidel,2001: Decadal change in the south tropical Pacific in a global assimilation analysis, Geophys. Res. Lett., 28, 3461-3464.

Chen, D., S. E. Zebiak, A. J. Busalacchi, and M. A. Cane, 1995: An improved procedure for El Nin˜o forecasting. Science, 269, 1699–1702.

—,—,— and A.J. Busalacchi, 1997: Initialization and Predictability of a Coupled ENSO Forecast Model, Monthly Weather Review, 125,773-788.

—, M. A. Cane, A. Kaplan, S. E. Zebiak and D. J. Huang, 2004: Predictability of El Niño over the past 148 years. Nature, 428(6984): 733-736.

Deng Z., Tang Y. and Zhou X., 2007: Reconstruction of historic wind stress over tropical Pacific for 1856-1947.

—,— and — , 2008: The retrospective prediction of ENSO from 1881-2000 by a hybrid coupled model – (I): SST Assimilation with Ensemble Kalman Filter.

Dewitte, B., S.-W. Yeh, B.-K. Moon, C. Cibot, and L. Terray, 2007: Rectification of ENSO Variability by Interdecadal Changes in the Equatorial Background Mean State in a CGCM Simulation. J. Climate,20,2002-2021.

Ebisuzaki, W., 1997: A method to examine the statistical significance of a correlation when the data are serially correlated, J. Climate, 10, 2147–2153,

Eckert, C., and M. Latif, 1997: Predictability of a stochastically forced hybrid coupled model of El Niño. J. Climate, 10, 1488–1504.

Flügel, M., P. Chang, and C. Penland, 2004: The role of stochastic forcing in modulating ENSO predictability. J. Climate, 17, 3125–3140.

Garreaud, R. D., and D. S. Battisti,1999: Interannual (ENSO) and in-terdecadal(ENSO-like) variability in the Southern tropospheric circulation, J.Clim., 12, 2113-2123 .

Gu, D., and S. G. H. Philander, 1997: Interdecadal climate fluctuation that depend on exchanges between the Tropics and the extratropics. Science, 275, 805–807.

Hasegawa, T. and K., Hanawa, 2003:, Decadal-scale variability of upper ocean heat content in the tropical Pacific. Geophysical Research Letters, 30(6), 1272.

Hunt, B. G. and Elliott, T. I.: 2003: 'Secular variability of ENSO events in a 1000-year climatic simulation', Clim. Dyn. 20, 689–703.

Ji, M., A. Leetmaa, and V. E. Kousky, 1996: Coupled model predictions of ENSO during the 1980s and the 1990s at the National Centers for Environmental Prediction. J. Climate, 9, 3105–3120.

Jin, J.-F., D. Neelin, and M. Ghil, 1994: ENSO on devil's staircase. Science, 264, 70-72.

Jin, F.-F., 1997: An equatorial ocean recharge paradigm for ENSO. Part I: Conceptual model. J. Atmos. Sci., 54,811-829.

—, and S. –I. An, 1999: Thermocline and zonal advective feedbacks within the equatorial ocean recharge oscillator model for ENSO. Geophys. Res. Lett., 26, 2989-2992.

John P. W., and Jeffrey B. W., 1999: Quantifying persistence in ENSO. J. Atmos. Sci., 56, 2737–2760.

Kalnay et al.,The NCEP/NCAR 40-year reanalysis project, Bull. Amer. Meteor. Soc., 77, 437-470, 1996.

Karspeck, A., A. Kaplan and M. Cane, 2006: Predictability loss in an intermediate ENSO model due to initial error and atmospheric noise. J. Climate, 3572-3588.

Kiem A.S. and S.W. Franks, 2004: Multi-decadal variability of drought risk, eastern Australia, Hydrol. Proc. 18 (11), pp. 2039–2050.

Kirtman, B. P., and Schopf, P. S., 1998: Decadal variability in ENSO predictability and prediction, J. Climate, 11, 2804-2822.

Kistler R., Coauthors, 2001: The NCEP–NCAR 50-year reanalysis: Monthly means CD-ROM and documentation. Bull. Amer. Meteor. Soc, 82, 247–268.

Kleeman, R. and McCreary, J. P. 1999:, A mechanism for generating ENSO decadal variability. Geophysical Research Letters, 12, 1743-1746.

—, and A. M. Moore, 1997: A theory for the limitation of ENSO predictability due to stochastic atmospheric transients. J. Atmos. Sci., 54, 753–767.

—, and S. B. Power, 1994: Limits to predictability in a coupled ocean–atmosphere model due to atmospheric noise. Tellus, 46A, 529–540.

Latif, M., D. Anderson, T. P. Barnett, M. A. Cane, R. Kleeman, A.Leetmaa, J. J. O'Brien, A. Rostati, and E. K. Schneider, 1998:TOGA review paper ''Predictability and Prediction.'' J. Geophys.Res., 103, 14 375–14 394.

Linsley, B. K., G. M. Wellington, and D. P. Schrag, 2000: Decadal sea surface temperature variability in the subtropical South Pacific from 1726 to 1997 A.D., Science, 290, 1145-1148.

Luo, J.-J. and T. Yamagata, 2001: Long-term El Ni$\tilde{n}$o-Southern Oscillation (ENSO)-like variation with special emphasis on the Souther Pacific. J. Geophys.Res., 106,22211-22227.

Madec, G., P. Delecluse, M. Imbard, and C. Levy, 1998: OPA 8.1 ocean general circulation model reference manual. Institut Pierre-Simon Laplace des Sciences l'Environnement Global, LODYC, Université Pierre et Marie Curie, Paris, France, 97pp.

Mantua, N. J., and S. R. Hare,2002:The Pacific Decadal Oscillation, J.Oceanogr., 58, 35-44.

McPhaden, M.J., 2003: Tropical Pacific Ocean heat content variations and ENSO persistence barriers. Geophys. Res. Lett., 30(9), 1480, doi:10.1029/2003GL016872

Monahan, A. H., 2001: Nonlinear principal component analysis: Tropical Indo-Pacific sea surface temperature and sea level pressure. J. Climate, 14, 219–233.

—, and A. Dai, 2004:The spatial and temporal structure of ENSO nonlinearity . J. Climate, 17 3026-3036.

Moore, A. M., and R. Kleeman, 1998: Skill assessment for ENSO using ensemble prediction. Quart. J. Roy. Meteor. Soc., 124,557–584.

— and —, 1999: Stochastic forcing of ENSO by the Intraseasonal Oscillation. J. *Climate,* **12,** 1199-1220.

—, Zavala-Garay, Y. Tang, R. Kleeman, J. Vialard, A. Weaver, K. Sahami, D. L. T. Anderson and M. Fisher 2006: Optimal Forcing Patterns for Coupled Models of ENSO J. Climate, 19, 4683-4699.

Münnich, M, M.A. Cane, and S.E. Zebiak, 1991: A study of self-excited oscillations of the tropical ocean-atmosphere system. II. Nonlinear cases, J. Atmos. Sci., 48, 1238-1248.

Nakaegawa, T. and M. Kanamitsu et al.,2004: Interdecadal trend of prediction skill in an ensemble AMIP-type experiment. American Meteorological Society. 7,2881-2889.

Penland, C. and L. Matrasova, 1994: A balance condition for stochastic numerical models with application to the El Ni˜no Suthern Oscillation. J. Climate, 7, 1352–1372.

Rodgers, K. B., P. Friederichs, and M. Latif, 2004: Tropical Pacific Decadal Variability and Its Relation to Decadal Modulations of ENSO J. Climate,17, 3761–3774.

Smith, T. M., and R. W. Reynolds, 2002: Bias corrections for historical sea surface temperatures based on marine air temperatures. J. Climate,15,73-87.

— and —, 2004: Improved extended reconstruction of SST (1954-1997). J. Climate, 17,2466-2477.

Solomon, A., J. P. McCreary, R. Kleeman, and B. A. Klinger, Interannual and decadal variability in an intermediate coupled model of the Pacific region, J. Clim., 16, 383-405, 2003.

Tang, Y., Z. Deng, X. Zhou, Y. Cheng and D. Chen, 2007: Interdecadal Variation of ENSO Predictability in Multiple Models. (submitted).

—, Kleeman, R., and Moore, A., 2005: On the reliability of ENSO dynamical predictions. J. Atmos. Sci., 62, 1770-1791.

—, Kleeman, R., and Moore, A., 2004a: SST assimilation experiments in a tropical Pacific Ocean model, J Phys. Oceangr. 34, 623-642.

—, — and —, 2004b; A simple method for estimating variations in the predictability of ENSO. Geophy. Res. Letters, 31, L17205 10.1029/2004GL020673

Thompson, C. J. and D. S. Battisti, 2000: A linear stochastic dynamical model of ENSO.Part I: Model development. J. Climate, 13, 2818–2832.

Timmerman, A., and F.-F. Jin, 2002: A nonlinear mechanism for decadal El Niño amplitude changes, Geophys. Res. Lett., 10.1029/2001GL013369.

Torrence, C. and G. P. Compo, 1998: A Practical Guide to Wavelet Analysis. Bull. Amer. Meteor. Soc., 79, 61-78.

Wang, B. 1995: Interdecadal changes in El Niño onset in the last four decades. J. Climate, 8, 267–285.

—, A. Barcilon, and Z. Fang, 1999: Stochastic dynamics of El Niño-Southern Oscillation. J. Atmos. Sci., 56, 5–23.

Yeh S.-W., J.-G. Jhun, I.-S. Kang, and B. P. Kirtman,2004, The Decadal ENSO Variability in a Hybrid Coupled Model . J. Climate,17, 1225–1238.

Yu, J. Y. and W. T. Liu, 2003: A linear relationship between ENSO intensity and tropical instability wave activity in the eastern Pacific Ocean, Geophys. Res. Lett., 30(14), 1735, doi:10.1029/2003GL017176.

Zhang, R.-H., L. M. Rothstein, and A. J. Busalacchi, Origin of upper-ocean warming and El Niño change on decadal scales in the tropical Pacific Ocean, Nature, 391, 879-882, 1998.

Zhang, R.-H., L. M. Rothstein, and A. J. Busalacchi, 1999: Interannual and decadal variability of the subsurface thermal structure in the Pacific Ocean: 1961-90. Climate Dynamics, 15: 703-717.

Zhang R. and A.J. Busalacchi, 2005: Interdecadal Change in Properties of El Niño–Southern Oscillation in an Intermediate Coupled Model. J. Climate, 18, 1369–1380.

—, S.E. Zebiak, R. Kleeman, and N. Keenlyside, 2005. Retrospective El Niño Forecasts Using an Improved Intermediate Coupled Model. Monthly Weather Review, 133,2777–2802

Zhou X.B., Tang Y. and Deng Z. 2007: Assimilation of Historic SST Data for ENSO Hindcast of the Past 126 Years. (submitted)

Table and Figure Captions

Table 1. The correlations coefficient between the correlation skill (CORR), and RMSE skill of predictions at 6-month lead and the variance of several decomposed components of NINO3 SSTA index, obtained using the 20-yr running scheme. The boldfaced numbers are the correlation coefficients with absolute value greater than 0.5, which is often considered as a useful skill.

FIG. 1. (a) Anomaly correlations and (b) RMSE between observed and predicted NINO3 index, as a function of lead time, for six consecutive 20-year periods from 1881-2000.

FIG.2. Time series of observed (grey line) and predicted (black line) NINO3 SSTA index at 6-month lead from 1881-2000.

FIG.3. (a) Anomaly correlation between observed and predicted NINO3 SSTA index (thick-solid line), at lead time of 6 months; the persistent correlation prediction skill at lead time of 6 months (thin-dashed line) and the variance of observed NINO3 index (thin-solid line). (b) Anomaly RMSE between observed and predicted NINO3 SSTA index at lead time of 6 months. All time series are obtained using the 20-yr running scheme.

FIG. 4. (a) The scattered plot of the correlation skill of predictions at 6-month lead against the variance accounted for by EOF1 (V_PC1) (circle) and against the variance of NINO3 SSTA index (asterisk). The solid (dashed) line was obtained by linear regression to fit the relationship of V_PC1 - Correlation skill (V_NINO3 – Correlation skill). (b) As in (a) but for RMSE.The variances were calculated using the 20-yr running scheme and normalized.

FIG.5. The wavelet power spectrum of (a) observed NINO3 SSTA index, (b) modeled NINO3 SSTA index and (c) Z20_Tilt. The contour levels are chosen so that 75%, 50%, 25%, or 5% of the wavelet power is above each level respectively. Black contour is the 10% significance level, using a red-noise (autoregressive lag(1)) background spectrum. The corresponding global wavelet power spectrum is shown in the right side (black line). The dashed line is the significance for the global wavelet spectrum, assuming the same significance level and background spectrum as in local wavelet spectrum.

FIG.6. The prediction skills of NINO3 SSTA index at the 6-month leads (thin line for correlation and dashed line for RMSE) and the variance of several decomposed NINO3 SSTA indices (think line), with the signals of (a) greater than 2 yr periods; (b) 2-4 yr periods and (c) less than 3 months. The normalization was performed for each variable for the comparison of different variables.

FIG.7. The simulation skill of the analyzed NINO3 SSTA index against the observed counterpart. (a) correlation and (b) relative RMSE (i. e., normalized by standard deviation of observed NINO3 SSTA index). The 20-yr running scheme was used in (a) and (b).

FIG.8. EOF1 of analyzed ocean variables for the past 120 yrs. (a) SSTA, (b) UA and (c) Z20A.

FIG.9. The variances explained by EOF1 mode for analyzed SSTA (thick line), UA (dashed line) and Z20A (thin line). The 20-yr running scheme was used for obtaining these variances.

Table 1. The correlations coefficient between the correlation skill (CORR), and RMSE skill of predictions at 6-month lead and the variance of several decomposed components of NINO3 SSTA index, obtained using the 20-yr running scheme. The boldfaced numbers are the correlation coefficients with absolute value greater than 0.5, which is often considered as a useful skill.

Period	>4yr	2-4yr	1-2yr	6-12Mth	3-6Mth	<3Mth
CORR	0.09	**0.74**	-0.40	0.02	-0.33	**-0.71**
RMSE	0.34	**-0.67**	0.43	0.13	**0.58**	**0.62**

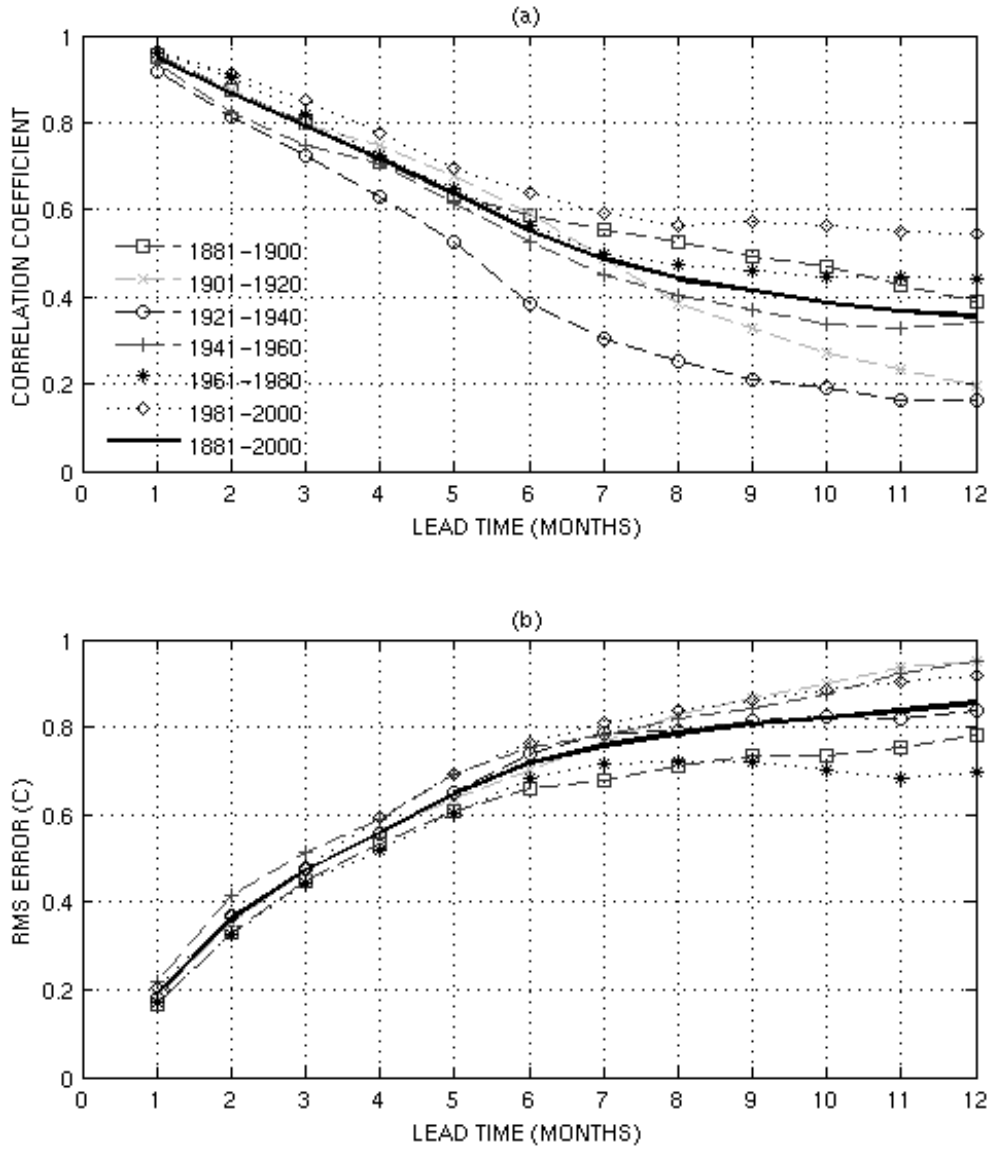

FIG. 1. (a) Anomaly correlations and (b) RMSE between observed and predicted NINO3 index, as a function of lead time, for six consecutive 20-year periods from 1881-2000.

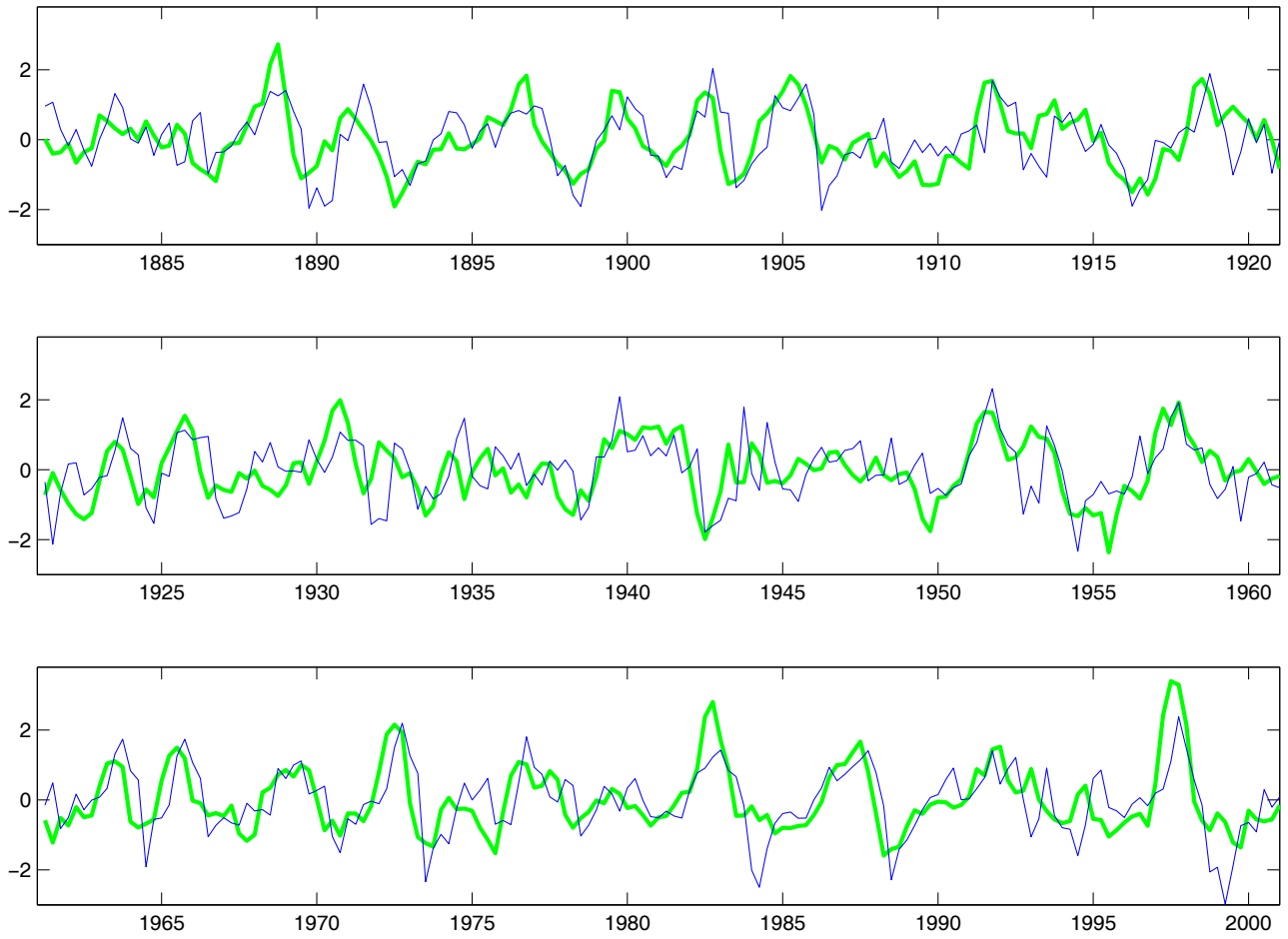

FIG.2. Time series of observed (grey line) and predicted (black line) NINO3 SSTA index at 6-month lead from 1881-2000.

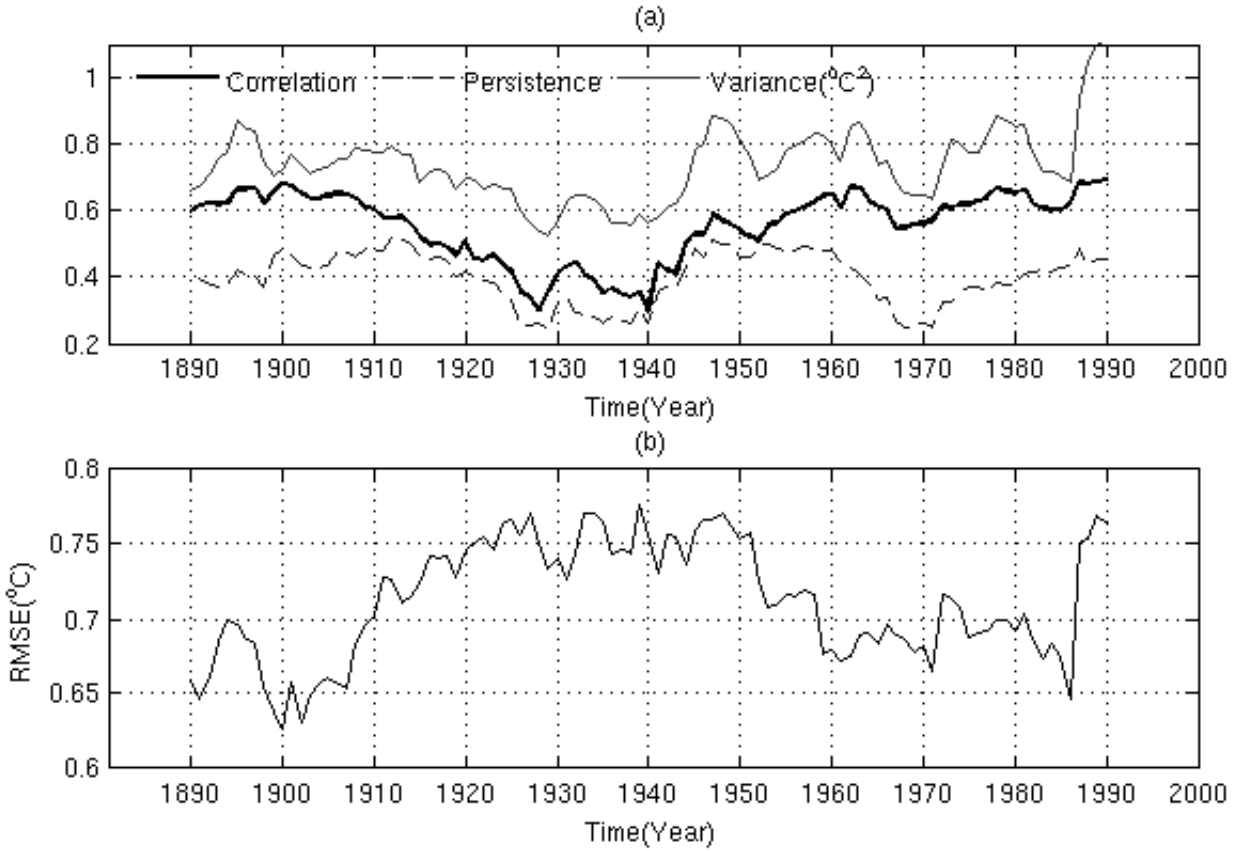

FIG.3. (a) Anomaly correlation between observed and predicted NINO3 SSTA index (thick-solid line), at lead time of 6 months; the persistent correlation prediction skill at lead time of 6 months (thin-dashed line) and the variance of observed NINO3 index (thin-solid line). (b) Anomaly RMSE between observed and predicted NINO3 SSTA index at lead time of 6 months. All time series are obtained using the 20-yr running scheme.

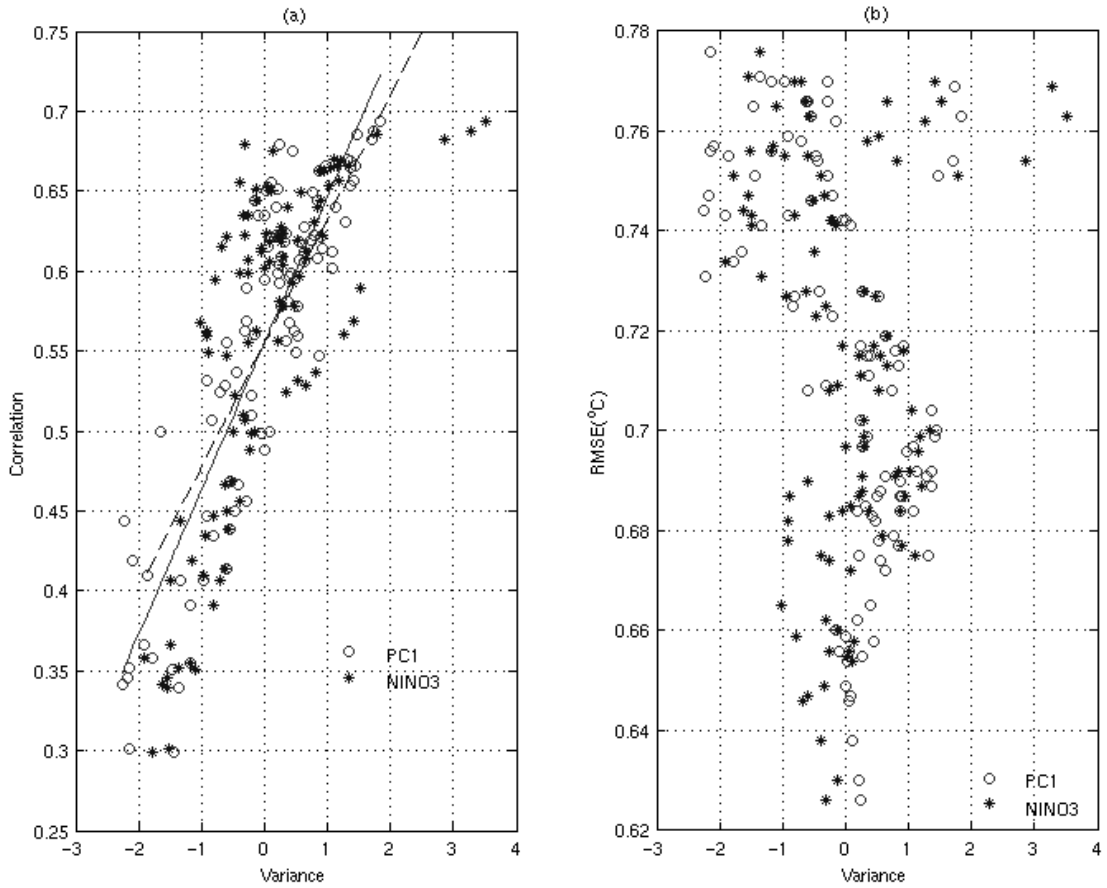

FIG. 4. (a) The scattered plot of the correlation skill of predictions at 6-month lead against the variance accounted for by EOF1 (V_PC1) (circle) and against the variance of NINO3 SSTA index (asterisk). The solid (dashed) line was obtained by linear regression to fit the relationship of V_PC1 - Correlation skill (V_NINO3 – Correlation skill). (b) As in (a) but for RMSE.The variances were calculated using the 20-yr running scheme and normalized.

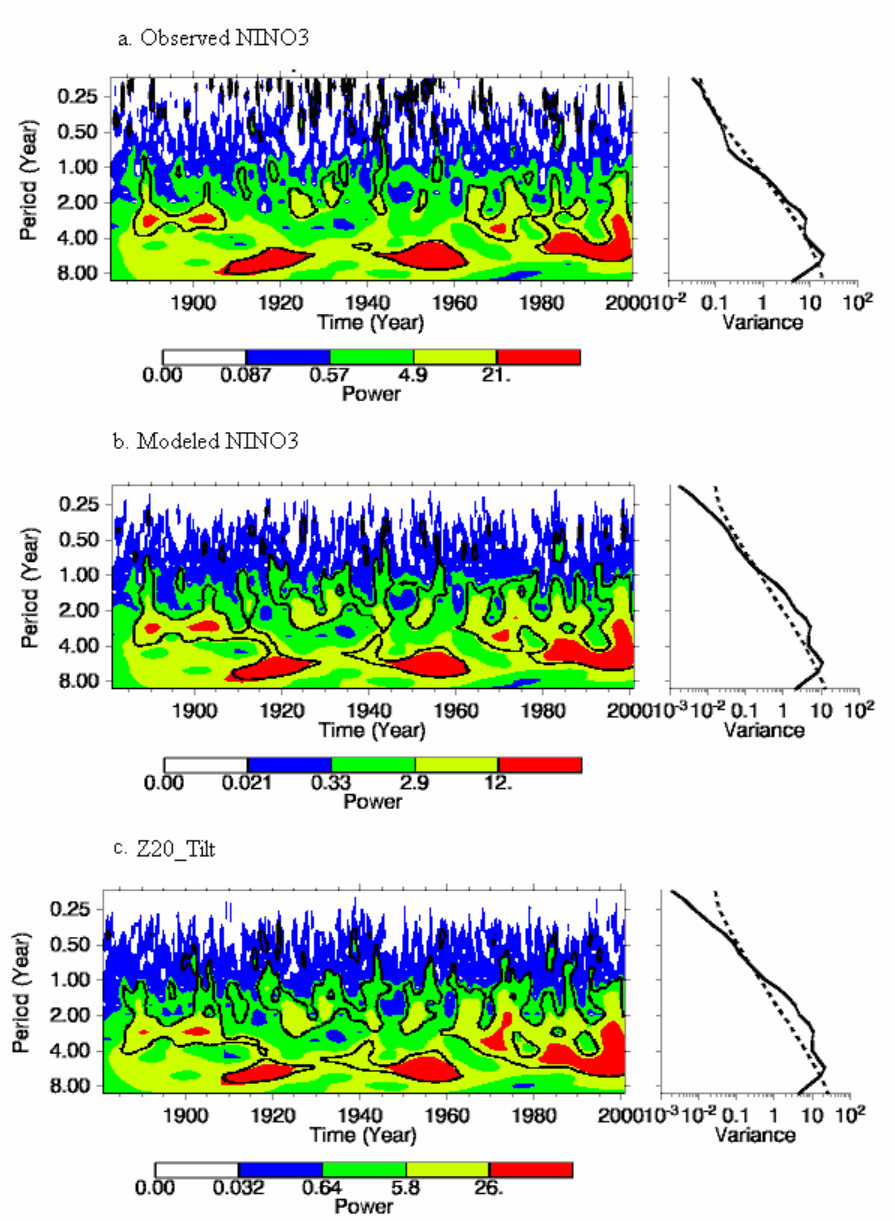

FIG.5. The wavelet power spectrum of (a) observed NINO3 SSTA index, (b) modeled NINO3 SSTA index and (c) Z20_Tilt. The contour levels are chosen so that 75%, 50%, 25%, or 5% of the wavelet power is above each level respectively. Black contour is the 10% significance level, using a red-noise (autoregressive lag(1)) background spectrum. The corresponding global wavelet power spectrum is shown in the right side (black line). The dashed line is the significance for the global wavelet spectrum, assuming the same significance level and background spectrum as in local wavelet spectrum.

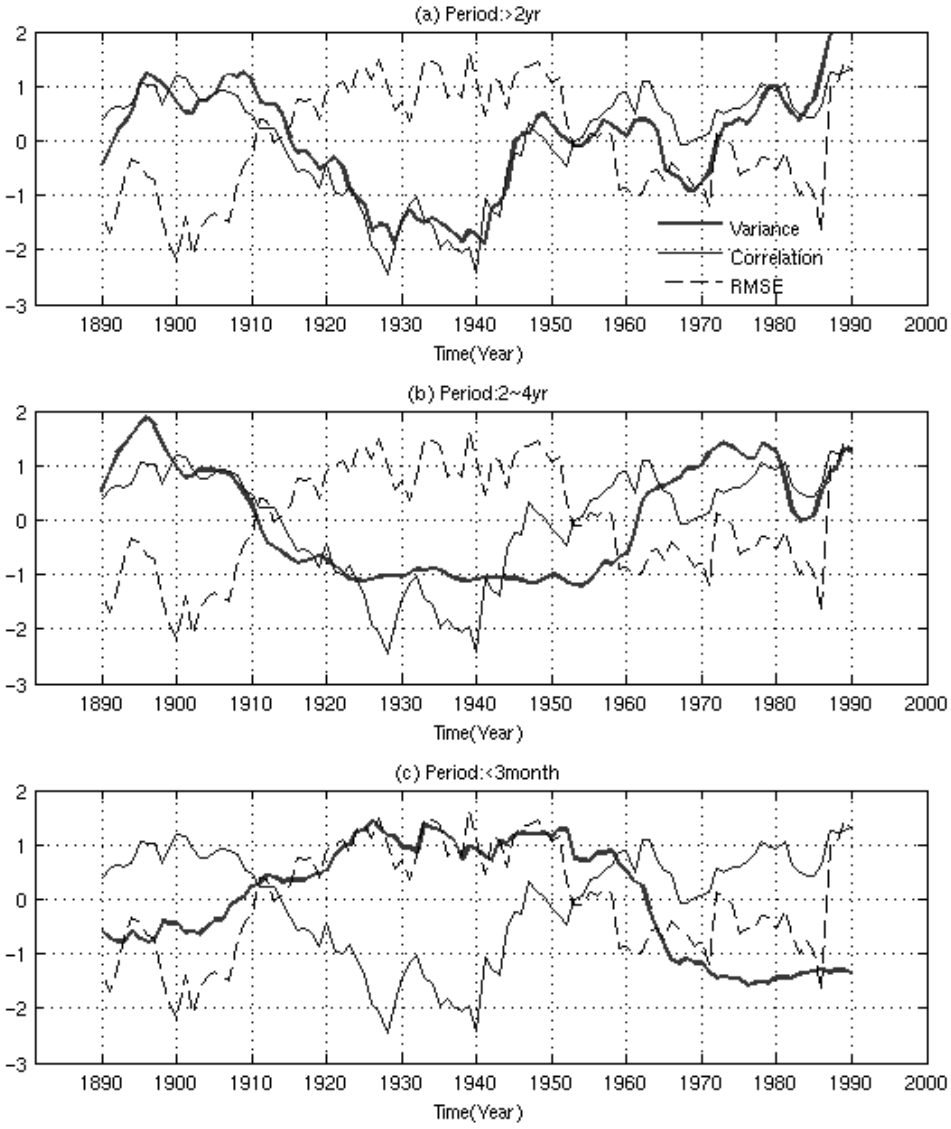

FIG.6. The prediction skills of NINO3 SSTA index at the 6-month leads (thin line for correlation and dashed line for RMSE) and the variance of several decomposed NINO3 SSTA indices (think line), with the signals of (a) greater than 2 yr periods; (b) 2-4 yr periods and (c) less than 3 months. The normalization was performed for each variable for the comparison of different variables.

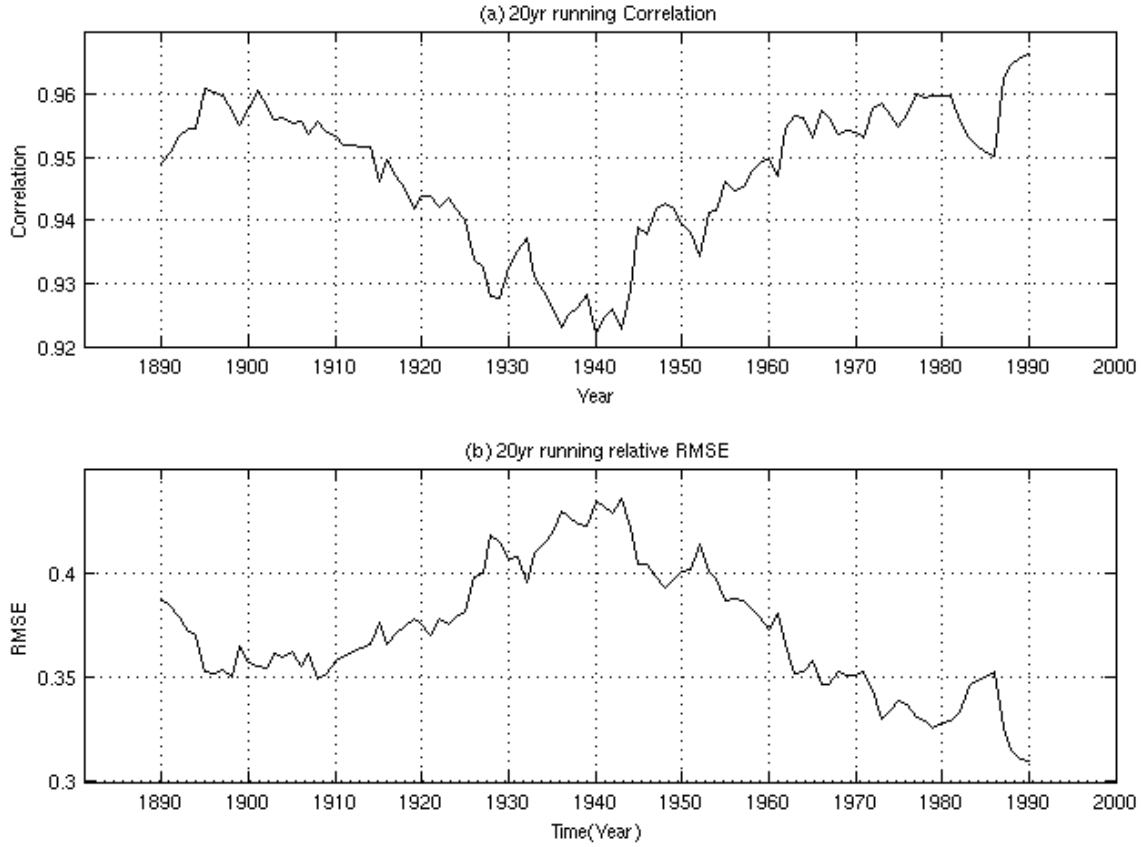

FIG.7. The simulation skill of the analyzed NINO3 SSTA index against the observed counterpart. (a) correlation and (b) relative RMSE (i. e., normalized by standard deviation of observed NINO3 SSTA index). The 20-yr running scheme was used in (a) and (b).

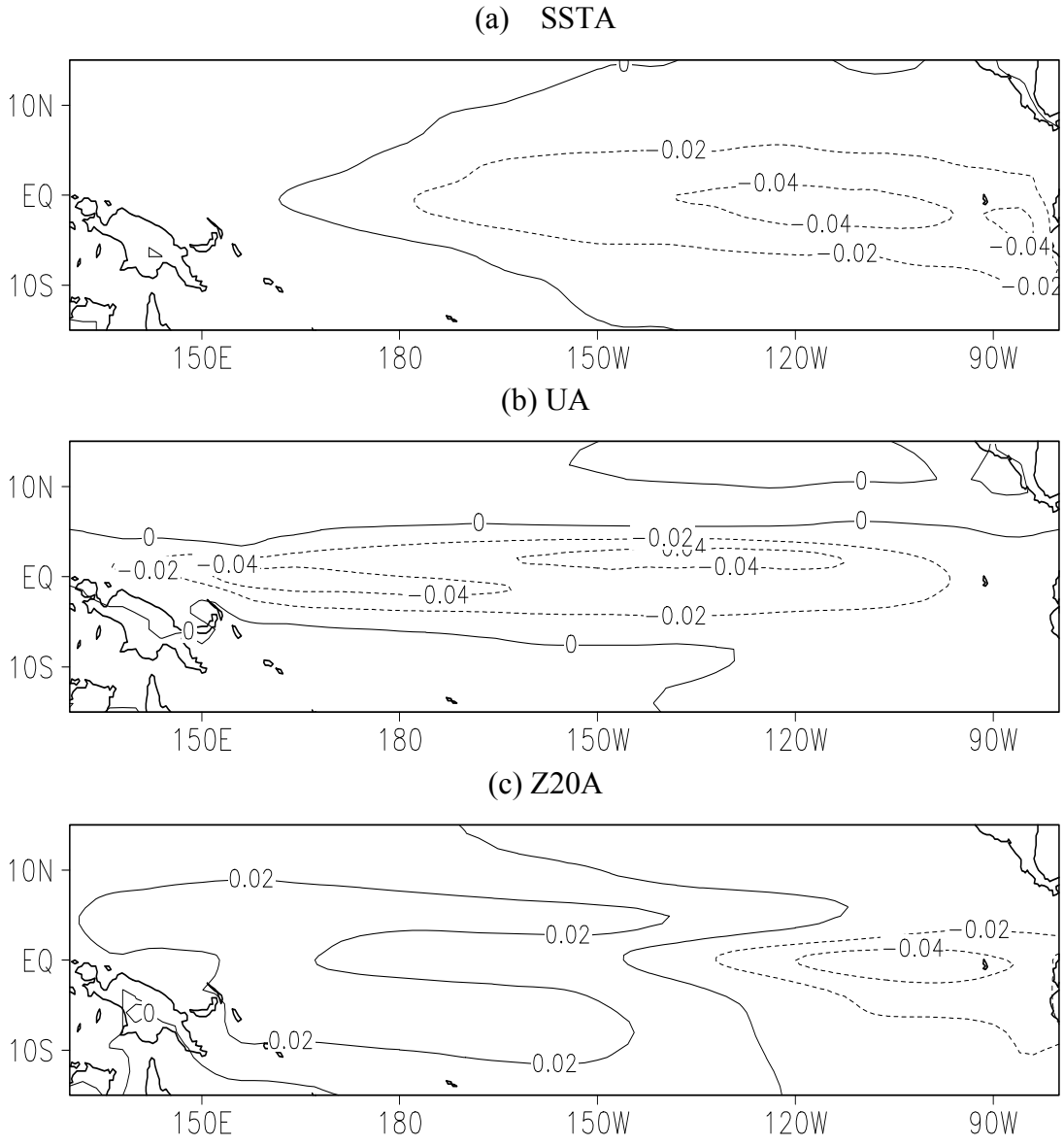

FIG.8. EOF1 of analyzed ocean variables for the past 120 yrs. (a) SSTA, (b) UA and (c) Z20A

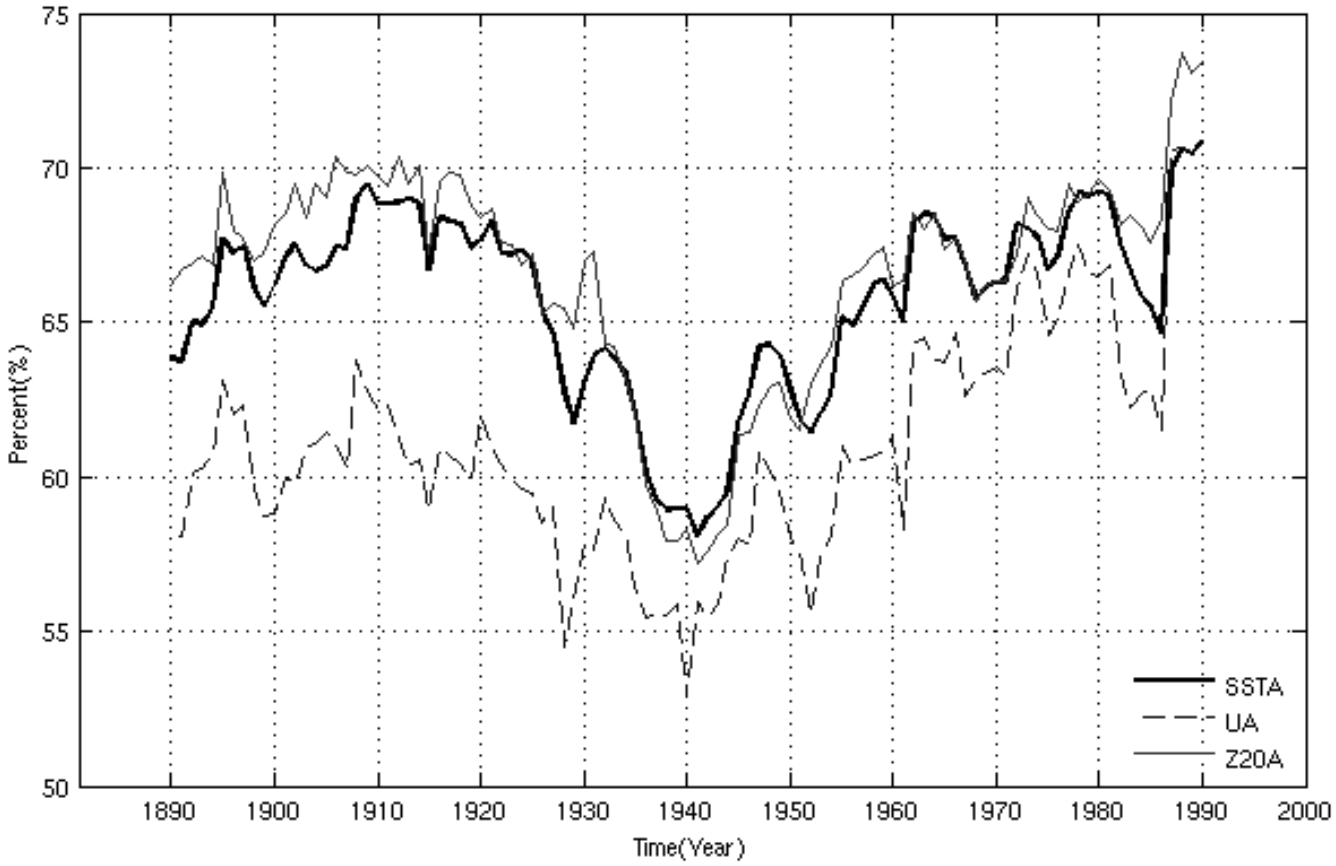

FIG.9. The variances explained by EOF1 mode for analyzed SSTA (thick line), UA (dashed line) and Z20A (thin line). The 20-yr running scheme was used for obtaining these variances.